

1 **Cardiac-generated sympathetic stress alters heart-brain communication, reduces EEG-**
2 **theta activity, and increases locomotor behavior**

3
4 *Jacopo Agrimi*^{a,b}, *Danilo Menicucci*^c, *Marco Laurino*^d, *Chelsea D Mackey*^b, *Laila Hasnain*^b, *Sneha*
5 *Dodaballapur*^b, *Ross A McDevitt*^h, *Donald B Hoover*^{e,g}, *Angelo Gemignani*^{*c}, *Nazareno Paolucci*^{*}
6 *^{a,f}, Edward G Lakatta^{*b}*

7 *a) Department of Medicine, Johns Hopkins University School of Medicine, Baltimore, MD, USA.*

8 *b) Laboratory of Cardiovascular Sciences, National Institute on Aging, National Institutes of*
9 *Health Biomedical Research Center (BRC), Baltimore, MD, USA*

10 *c) Department of Surgical, Medical, Molecular Pathology, and Critical Care Medicine,*
11 *University of Pisa, Pisa, Italy*

12 *d) Institute of Clinical Physiology, National Research Council, Pisa, Italy*

13 *e) Department of Biomedical Sciences, James H. Quillen College of Medicine, East Tennessee*
14 *State University, Johnson City TN.*

15 *f) Department of Biomedical Sciences, University of Padova, Padova, Italy*

16 *g) Center of Excellence in Inflammation, Infectious Disease and Immunity, East Tennessee*
17 *State University, Johnson City, TN*

18 *h) The Comparative Medicine Section, National Institute on Aging, National Institutes of*
19 *Health, Baltimore, MD, USA.*

20 **Contributed equally*

21 **Keywords:** Adenylyl cyclase type 8, EEG Theta Rhythm, Granger Causality, Locomotor Activity,
22 Heart-Brain Communication, Sympathetic Stress

23 Correspondence to:

24 **Nazareno Paolucci, M.D., Ph.D.**

25 Division of Cardiology, Traylor 911

26 Johns Hopkins Hospital

27 720 Rutland Avenue

28 Baltimore, MD, 21212

29 npaoloc1@jhmi.edu

30 **Edward G. Lakatta, M.D.**

31 Laboratory of Cardiovascular Sciences,

32 National Institute on Aging,

33 National Institutes of Health Biomedical Research Center (BRC),

34 Baltimore, MD, 21224

35 lakattae@grc.nia.nih.gov

36 **Abstract**

37 Brain modulation of myocardial activity via the autonomic nervous system is increasingly well
38 characterized. Conversely, how primary alterations in cardiac function, such as an intrinsic increase
39 in heart rate or contractility, reverberate on brain signaling/adaptive behaviors - *in a bottom-up*
40 *modality* - remains largely unclear. Mice with cardiac-selective overexpression of adenylyl cyclase
41 type 8 (TGAC8) display increased heart rate and reduced heart rhythm complexity associated with
42 a nearly abolished response to external sympathetic inputs. Here, we tested whether chronically
43 elevated intrinsic cardiac performance alters the heart-brain informational flow, affecting brain
44 signaling and, thus, behavior. To this end, we employed dual lead telemetry for simultaneous
45 recording of EEG and EKG time series in awake, freely behaving TGAC8 mice and wild-type (WT)
46 littermates. We recorded EEG and EKG signals, while monitoring mouse behavior with established
47 tests. Using heart rate variability (HRV) *in vivo* and isolated atria response to sympathomimetic
48 agents, we first confirmed that the TGAC8 murine heart evades autonomic control. The EEG
49 analysis revealed a substantial drop in theta-2 (4-7 Hz) activity in these transgenic mice. Next, we
50 traced the informational flow between EKG and EEG in the theta-2 frequency band via the Granger
51 causality statistical approach and we found a substantial decrement in the extent of heart/brain
52 bidirectional communication. Finally, TGAC8 mice displayed heightened locomotor activity in
53 terms of behavior, with higher total time mobile, distance traveled, and movement speed while
54 freezing behavior was reduced. Increased locomotion correlated negatively with theta-2 waves
55 count and amplitude. Our study shows that cardiac-born persistent sympathetic stress disrupts
56 the information flow between the heart and brain while influencing central physiological patterns,
57 such as theta activity that controls locomotion. Thus, cardiac-initiated disorders, such as
58 persistently elevated cardiac performance that escapes autonomic control, are penetrant enough
59 to alter brain functions and, thus, primary adaptive behavioral responses.

60

61

62

63

64 **Introduction**

65 According to the somatic marker theory postulated by Antonio Damasio (following the thoughts
66 of one of the fathers of psychophysiology, William James), afferent somatic signals arising from
67 the body's peripheral districts are integrated into higher brain regions, particularly the
68 ventromedial prefrontal cortex (VMPFC), and they can influence complex behaviors, such as
69 decision making^{1,2}. The bidirectional relationship between the heart and the brain falls entirely
70 within this loop. Indeed, besides the autonomic nervous system's descending control on cardiac
71 function, information is processed by the intrinsic cardiac nervous system (the so-called "little
72 brain of the heart") that communicates back to the brain through ascending fibers located in the
73 spinal cord and vagus nerve³. These afferent impulses reach relay stations such as the medulla,
74 hypothalamus, thalamus, and, ultimately, the cerebral cortex³, carrying sensory information that
75 can initiate centrally-directed behaviors⁴.

76 Cardiac rhythmicity is under continuous surveillance and control of the two branches of
77 the autonomic nervous system (ANS)⁵. A balanced influence of sympathetic and parasympathetic
78 efferent fiber discharge over cardiac pacemaker cells located in the sinoatrial and atrioventricular
79 nodes is ultimately needed to generate the final heart beating frequency (HR)⁵. However, there
80 are clinical situations in which the heart escapes this autonomic control. In this sense, the
81 transplanted heart that harbors severed efferent and afferent autonomic fibers is emblematic in
82 that it evades both sympathetic and parasympathetic surveillance almost entirely⁶. These
83 individuals experience persistently elevated HR at rest and cannot adjust their myocardial
84 performance to an increased workload, such as during exercise⁷. What is more, after heart
85 transplantation, 63% of heart recipients face anxiety and depression, especially during the first
86 post-transplant year⁸. Despite numerous observational clues suggesting that peripheral changes
87 in cardiac activity can influence behavior, definitive experimental evidence proving this point is
88 lacking, along with the nature of the mechanism(s) eventually underlying this *bottom-up*
89 phenomenon and most behavioral patterns that are affected⁹.

90 Transgenic mice that overexpress adenylyl cyclase (AC) type 8 (TGAC8) in a cardiac-
91 selective manner display persistent elevated HR, reduced HR variability (HRV), and increased

92 contractility owing to enduringly high intrinsic cardiac cAMP-PKA-Ca²⁺ signaling^{10,11}. The TGAC8
93 heart flees top-down autonomic surveillance by blocking beta-adrenergic signaling and
94 catecholamine production to escape harmful additional sympathetic stress. In the present study,
95 we sought to determine whether persistent cardiac-initiated stress also disrupts bottom-up
96 signaling from the heart to the brain, leading to altered brain activity and behavioral sequelae.

97 **2. Materials and Methods**

98 **2.1 Animals**

99 All studies were executed in agreement with the Guide for the Care and Use of Laboratory Animals
100 published by the National Institutes of Health (NIH Publication no. 85-23, revised 1996). The
101 experimental procedures were approved by the Animal Care and Use Committee of the National
102 Institutes of Health (protocol #441-LCS-2016). A breeder pair of TG^{AC8} mice, generated by ligating
103 the murine α -myosin heavy chain promoter to a cDNA coding for human AC8¹¹, were a gift from
104 Nicole Defer/Jacques Hanoune, Unite de Recherches, INSERM U-99, Hôpital Henri Mondor, F-
105 94010 Créteil, France. Wild type (WT) littermates, bred from the C57BL/6 background, were used
106 as controls.

107 **2.2 Evaluation of isolated atrial function and response to adrenergic agents**

108 To evaluate adrenergic responses of the sinoatrial node (SAN) in the absence of autonomic inputs,
109 we isolated the cardiac atria leaving the SAN intact. TGAC8 and control mice were deeply
110 anesthetized with isoflurane and euthanized by decapitation. Hearts were removed rapidly and
111 transferred to oxygenated (95% O₂, 5% CO₂), cold (4°C) Krebs-Ringer bicarbonate buffer (pH 7.35
112 to 7.4) of the following composition (mM): 120 NaCl, 4.7 KCl, 1.2 KH₂PO₄, 25 NaHCO₃, 2.5 CaCl₂,
113 1.2 MgCl₂, and 11.1 D-glucose. The entire atrium was dissected from the ventricles, and each side
114 was impaled with a small metal hook (#28 trout hooks) with attached 5-0 sutures. The left atrium
115 was anchored to the bottom of a vertical support rod in a 15 mL tissue bath, and the right atrium
116 was attached to a 25-g force transducer (World Precision Instruments, Sarasota, FL). Krebs-Ringer
117 buffer in the tissue bath was oxygenated continuously and maintained at 37°C. Spontaneous
118 atrial contractions were recorded at a resting tension of 0.3 to 0.5 g using a ML224 Bridge
119 Amplifier (ADInstruments, Colorado Springs, CO), a PowerLab/8SP, and a computer running Lab

120 Chart version 7.3.8. Buffer was replaced at 10 min intervals, and three times after recovery from
121 drug treatment. Baseline atrial rate and force of contractions were recorded after a 30 min
122 stabilization period. Then responses to a maximally effective concentration of the tyramine (10-4
123 M final concentration), which stimulates release of norepinephrine from noradrenergic nerves,
124 and the directly acting sympathomimetic, L-isoproterenol, were recorded¹². Treatments were
125 separated by at least 30 min to preclude desensitization.

126 2.2.1 Drugs

127 L-isoproterenol hydrochloride and tyramine hydrochloride were purchased from Sigma-Aldrich
128 (St. Louis, MO).

129 2.3 Telemetry double implant to simultaneously monitor the EEG and EKG

130 Telemetric radio transmitters (F20-EET; Data Sciences International (DSI), St. Paul, MN) were
131 surgically implanted in young (3-4 months) WT and TG^{AC8} mice as described¹³. Briefly two surface
132 electrodes, a positive electrode (parietal cortex; AP, -2.0 mm; L, 2.0 mm) and a reference electrode
133 (cerebellum; AP, -6.0 mm; L, 2.0 mm), were passed subcutaneously to the cranial base and placed
134 directly on the dura mater. Two additional bipotential electrodes were routed subcutaneously via
135 a vertical midline incision overlying the abdomen with leads situated in the right upper chest and

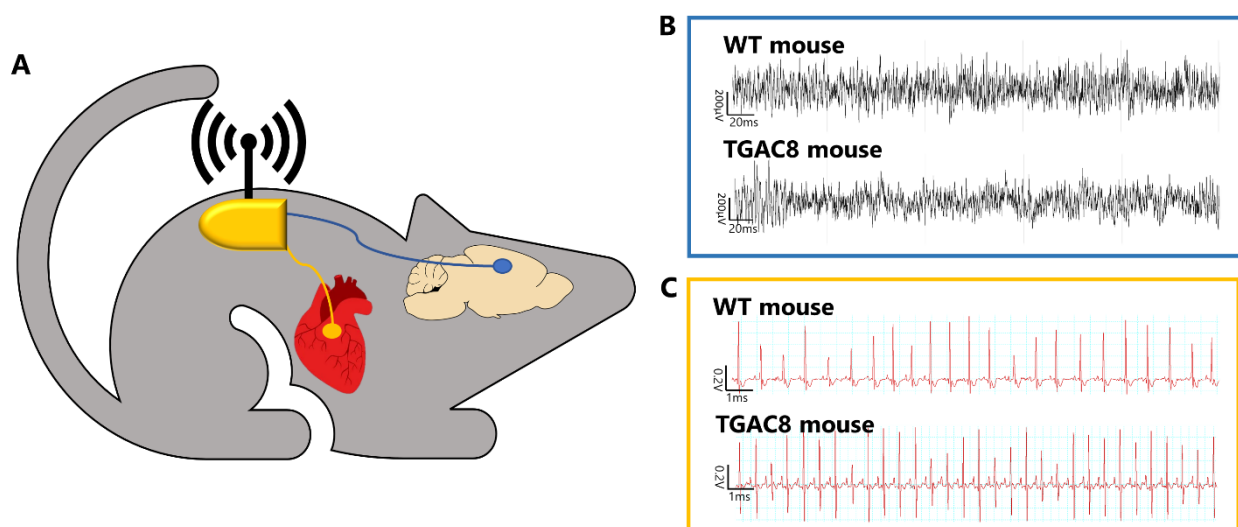


Figure 1 (A) Schematic of F20-EET double implant for telemetry recording in mice. (B) Representative images of EEG recording in a WT and TGAC8 mouse. (C) Representative images of EKG recording in a WT and TGAC8 mouse.

136 lower left abdomen below the heart to monitor continuous heart rate (Fig.1). Following a two-
137 weeks recovery period, 24-hr free behaving electrocardiogram (EKG) and electroencephalogram
138 (EEG) were recorded at a sampling rate of 1000 Hz and 500 Hz, respectively, with simultaneous
139 activity recording using the Dataquest A.R.T acquisition system (DSI, version 4.36). Average
140 activity counts were obtained every 10s.

141 **2.4 Signal analysis**

142 **2.4.1 EKG analysis**

143 Scoring of wake-sleep states (NeuroScore, DSI, version 3.2.0) allowed selecting all 10 seconds
144 wake epochs and extracting signals.

145 After appropriate pre-processing (see Supplemental Information), the series of heart beat time
146 intervals (RR series) was processed to derive HRV features. All features were signal-length
147 independent¹⁴ estimated on 10 seconds epochs to account for highly frequent wake/sleep
148 switches, thus describing the short-time heartbeat dynamics.

149 More in detail, we considered: mean value of RR intervals and, from frequency spectrum analysis
150 (Hamming-windowed FFT), the power in low frequency (LF: 0.15–1.5 Hz) and high frequency (HF:
151 1.5–4 Hz) bands. We also estimated some nonlinear features that provide additional information
152 about cardiac dynamics. According to previous works studying non-linearity in a heartbeat
153 series¹⁰, we characterize the RR series auto similarity through the Detrended Fluctuation Analysis
154 (DFA).

155 **2.4.2 EEG Spectral analysis**

156 For each 10 seconds wake epoch, a spectral analysis was performed on the EEG signal. The mean
157 power spectrum density characterizing wake state of each animal was evaluated by applying a
158 Hamming-windowed Fast Fourier Transform (FFT) and averaging them. Power values were
159 measured in dB, thus data from FFT were log-transformed. The activity in the theta-2 band (4-7
160 Hz) was estimated by averaging the bins belonging to the band.

161 **2.4.3 Theta wave recognition**

162 The theta wave recognition was carried out following the approach proposed and validated by
163 Ferrarelli and colleagues¹⁵ for sleep spindles, with some adaptations, as detailed in the SI. Three
164 parameters were derived from all detected events: the rate, peak amplitude, and dominant
165 frequency. The rate corresponded to the number of events per time unit, and the peak amplitude
166 was defined as the local maximum of each theta wave event. The dominant frequency is the
167 average of 4-7 Hz frequencies weighted by the associated squared coefficients of the discrete
168 Fourier transform. Measures characterizing each animal were derived as the average overall theta
169 wave events detected during its wake epochs.

170 **2.5 Brain/heart communication**

171 The brain/heart communication study was based on a Granger Causality (GC) analysis. $GC_{x \rightarrow y}$ is a
172 measure of the contribution of the past of the $x(t)$ time-series to the prediction of the present
173 value of $y(t)$, compared to the contribution of the past of the $y(t)$ *time series* in the prediction of
174 its own present value. In our application (Fig. 5) $x(t)$ and $y(t)$ are signals related to brain and heart
175 functioning and the GC has allowed estimating heart rhythm influence on brain EEG rhythms and
176 vice versa (by switching x and y). Specifically, our analysis takes advantage of the variability
177 expressed over time by both the brain theta rhythm and heart rhythm and checks whether
178 amplitude variations of the former are predictive of changes in the latter or vice versa. For the
179 variability over time of the theta rhythm, we used the amplitude of the envelope of the theta-
180 filtered signal (see supplementary data, steps 1 and 2 in the theta wave recognition procedure),
181 whereas the heart rhythm variability was directly expressed in the tachogram. To perform the GC
182 analysis, both series were interpolated at the same frequency (10 Hz). The GC analysis was
183 conducted using the Causal Connectivity Toolbox¹⁶, which assumes a linear model and order
184 within the model, estimated using the Akaike Information Criterion. Herein, in unison with the GC
185 applicability criteria, EEG epochs satisfying the stationarity test¹⁷ were retained for the analysis
186 (more than 95% retained). For each mouse, the median of their epochs model orders was chosen
187 as the representative order. The 95th percentile of 'animals' model orders was taken as the overall
188 order¹⁸: from data collected in this experiment, this corresponded to 20 samples, equivalent to 2
189 seconds. The overall model order was applied to the GC estimates of all wake epochs for all mice
190 (both groups). Finally, the validity of the model order was verified by estimating the model

191 consistency (percentage of data correlation structure explained by the model)¹⁹. Consistency
192 values higher than 75% were considered satisfactory and all periods had mean consistencies of
193 90% or above.

194 **2.6 Behavioral tests**

195 **2.6.1 Open field**

196 Open field (OF) is a gold standard behavioral test used to study locomotor activity, exploratory
197 behavior, and anxiety-like behavior in rodents ²⁰. The animal is free to explore a circumscribed
198 environment (50cm x 50cm arena surrounded by walls), and its locomotor activity and its tendency
199 to explore open spaces or hide in the peripheral corners of the arena is evaluated. The analysis of
200 the behavioral parameters has been performed using ANY-maze software (Stoelting Co., IL, USA).

201 **2.6.2 Elevated plus maze**

202 Elevated plus maze (EPM) is another consolidated test to study anxiety-like behavior and
203 locomotor activity in rodents. Elevated Plus Maze test exploits the rodent's conflict between
204 aversion to open spaces (i.e., hides in closed arms of a labyrinth) and instinct to explore new
205 environments (e.g., exploration of open arms of the same labyrinth) ²⁰. The analysis of the
206 behavioral parameters has been performed employing ANY-maze.

207 **2.6.3 Light-Dark Box**

208 The light/dark box (LDB) test is based on the innate aversion of mice to illuminated spaces and
209 the spontaneous exploratory activity in response to minor stressors, such as a new environment
210 and light. This experimental task allows for evaluation of the level of anxiety-like behavior
211 experienced by the animals. The test apparatus consists of a small dark compartment and a larger
212 illuminated compartment²¹. The analysis of the behavioral parameters has been performed
213 through ANY-maze software.

214 **2.6.4 Fear Conditioning Test**

215 The fear conditioning (FC) test measures the capacity of rodents to learn and recall an association
216 between environmental cues and aversive experiences. In this paradigm, mice are placed into a

217 conditioning chamber and are given pairs of a neutral auditory stimulus and an aversive stimulus
218 (electric foot shock). After the conditioning acquisition, 24 hours later, the mice are exposed to
219 the identical chamber and a differently shaped space with the presentation of the auditory cue.
220 Freezing behavior during the test is recorded as an index of associative learning²².

221 2.6.5 Y-Maze

222 Y-Maze allows studying spatial memory in rodents. The test stems from the tendency the rodents

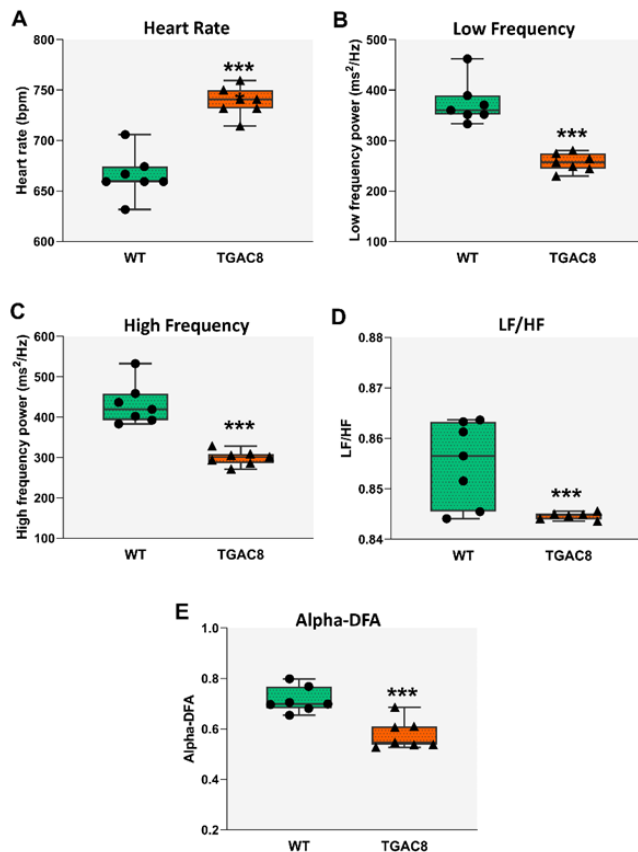


Figure 2 Heart rate variability is impaired in TGAC8 mice. (A-E) Heart Rate Variability measured *in vivo* from telemetric EKG recording. (A) Heart Rate; (B) Low Frequency; (C) High Frequency; (D) Low Frequency/High Frequency ratio; (E) Alpha-Detrended Fluctuation Analysis. Results are shown as box and whiskers plot; N=7, unpaired t-test; ***p<0.001

have to explore new environments, preferring a labyrinth arm that is not yet explored to an already known one²³. The analysis of the behavioral parameters has been performed using ANY-maze software.

2.7 Statistical analysis procedures

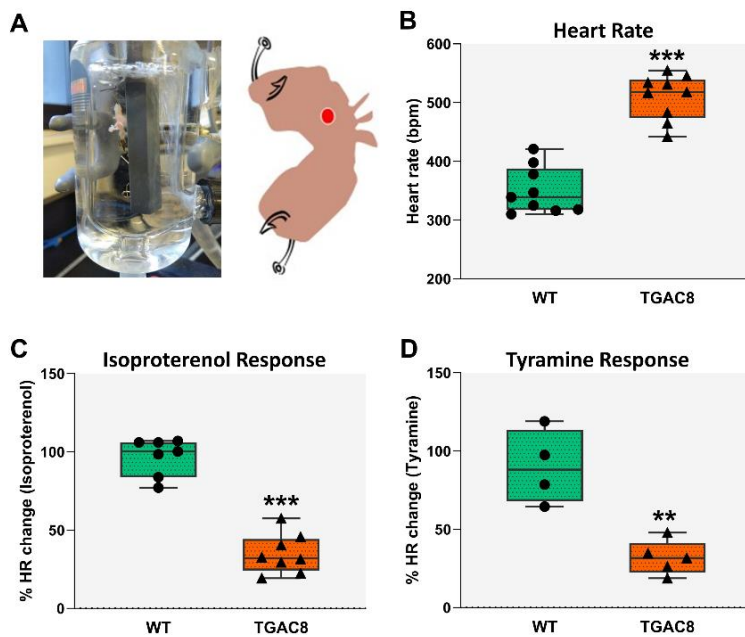
Results are presented as box-and-whisker plots (the box extends from the 25th to 75th percentiles, the median value is depicted by the line in the middle of each box, the whiskers go down to the 1th percentile and up to the 99th). All parametric data were analyzed by unpaired t-test between the WT and TGAC8 groups.

Correlations between groups of values were evaluated through Pearson's coefficient, P-value <0.05 was considered statistically significant.

241 3. Results

242 3.1 The heart escapes autonomic surveillance in mice over-expressing AC8

243 Overexpressing AC8 in the SA node cells renders the heart unresponsive to ANS surveillance¹⁰.
 244 Here, we validated and expanded this evidence. Indeed, we first observed that the persistently
 245 elevated *in vivo* HR found in TGAC8 mice (**Fig. 2A**) goes hand-in-hand with a marked drop in both
 246 time domains and high- and low-frequency domain HR variability and their ratio recorded by the
 247 EKG branch of the double telemetry implant ($p < 0.001^{***}$ TGAC8 vs. WT) (**Fig. 2B-D**). The
 248 Detrended Fluctuation Analysis alpha (alpha-DFA) confirmed such evidence. Indeed, HR in TGAC8
 249 mice is less influenced by external systems compared to the WT counterparts ($p < 0.001^{**}$ TGAC8
 250 vs. WT) (**Fig.2E**).



We assessed the intrinsic response of the SAN to external sympathetic input in isolated atria, having an intact SAN. The basal beating rate of isolated atria from TGAC8 was markedly increased (**Fig.3B**) and there was a substantially decreased response to sympathomimetic agents, namely isoproterenol and tyramine (**Fig.3 C, D**). In aggregate, these data confirm that the cardiac pacemaker activity in TGAC8

262
 Figure 3 TGAC8 mice show a blunted response to sympathomimetic agents. Results from studies conducted in isolated mouse atria. (A) Representative picture and diagram of isolated atria preparation; (B) Heart Rate, $n=9$; (C) Change (in percentage) of heart rate after Isoproterenol administration $n=7-8$; (D) Change (in percentage) of heart rate after Tyramine administration, $n=4-5$. Results are shown as box and whiskers plot; unpaired *t*-test has been performed between WT and TGAC8 groups, $***p < 0.001$.

escapes external sympathetic control. Therefore, this mouse strain represents a valuable model to evaluate the functional

267 repercussions of possible alterations in heart-brain communication.

268 3.2 TGAC8 mice show lower EEG theta-2 power and decreased theta waves count and 269 amplitude

270 Next, we analyzed the EEG recordings to address the core hypothesis of the work, i.e., persistent
271 cardiac-initiated stress can influence brain signaling in a bottom-up modality. We first analyzed
272 all EEG power spectrum, comparing each *hertz* (1-50) in WT and TGAC8 mice (**Fig. 4A**). Cardiac-
273 selective AC8 overexpression significantly decreased the power in the range of theta-2 frequency

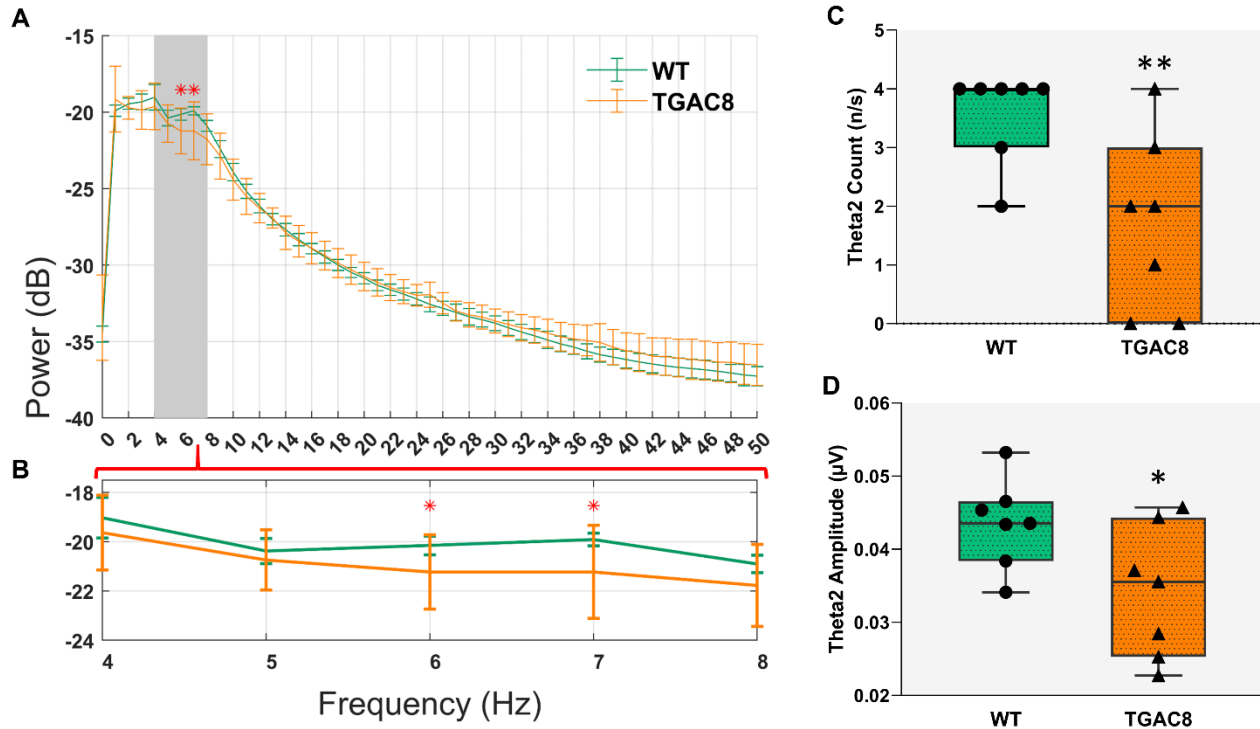


Figure 4 TGAC8 mice display an overall reduction in theta-2 activity. (A) Power spectrum 1-50 Hz; (B) Power spectrum, zoom on the theta-2 range; (C) Theta-2 waves count; (D) Theta-2 waves amplitude. Results in A and B are shown as mean and SD, in C and D as box and whiskers plot, N=7, unpaired t-test has been performed between WT and TGAC8 groups, * $p < 0.05$, ** $p < 0.01$.

274 (6-7 Hz) (**Fig. 4A, B**). These changes in theta-2 activity were not limited to the power spectrum
275 but also involved waves counts (-50% ** $p = 0.01$) and amplitude (* $p < 0.05$), all markedly reduced in
276 the TGAC8 mice (**Fig. 4C, D**). Thus, AC8 myocardial overexpression leads to a pronounced
277 downregulation of the theta-2 activity.

278 3.3 AC8 cardiac-selective overexpression impairs the brain-heart flow of information

279 To further prove that the alterations in EEG theta-2 frequency and patterns are related to the
 280 cardiac-initiated sympathetic stress experienced by the TGAC8 mice, we finally applied the GC
 281 analysis, a statistical approach that estimates causality between two time series, to evaluate the
 282 bidirectional flow of information between the heart and the brain²⁴. Herein, it enabled us to predict
 283 how cardiac rhythm can influence EEG frequencies and vice versa, thus providing a metric for the
 284 bidirectional flow of information between the two systems (**Fig. 5A**). In the range of theta-2, we

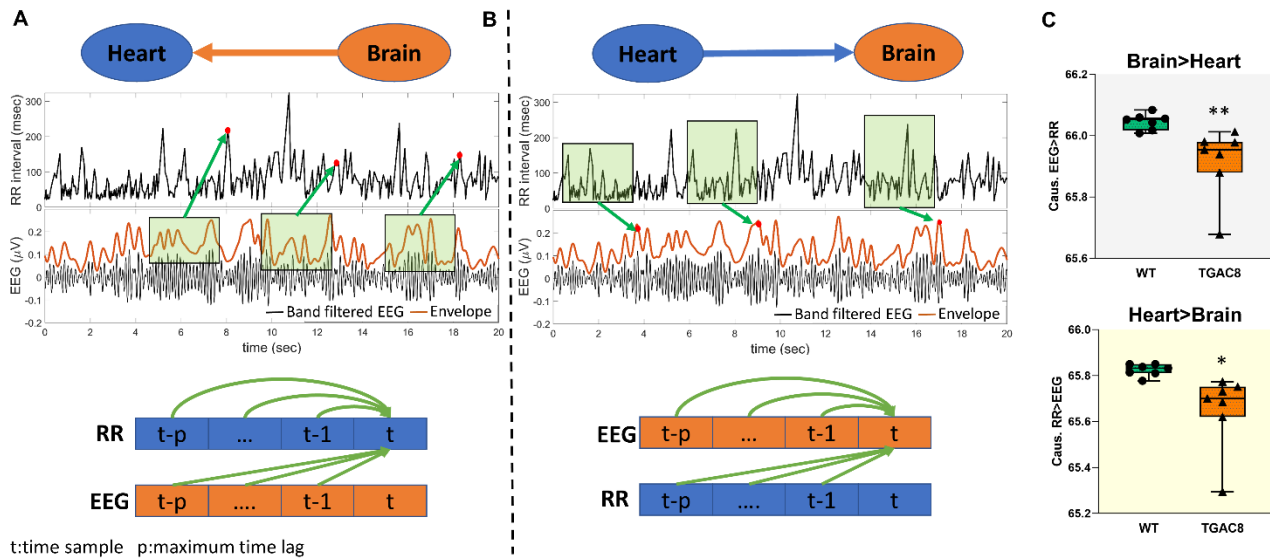


Figure 5. TGAC8 mice show an impairment in the heart-brain flow of information. **A. GC brain->heart estimate.** Amplitude of the envelope of the theta-filtered EEG signal (local amplitude) was extracted and used to estimate its contribution in the prediction of the heart rate variability (HRV). The box over the envelope signal depicts the length of past values in the time series used in the GC analysis to predict current HRV series. To derive the GC brain->heart, this predictive contribution was compared with that made by past values of the HRV series on its own current value. **B. GC heart->brain estimate.** HRV time-series was extracted and used to estimate its contribution in the prediction of the local amplitude of theta-filtered EEG signal. The box over the HRV time series depicts the length of past values in the time series used in the GC analysis to predict current theta amplitude. To derive the GC heart->brain, this predictive contribution was compared with that made by past values of the theta amplitude series on its own current value. **C.** dispersion within groups of GC estimates both for heart->brain and brain->heart directions. Results in C are shown as box and whiskers plot, N=7, unpaired t-test has been performed between WT and TGAC8 groups, *p<0.05, **p<0.01.

285 found significant impairment of the flow of information between the heart and the brain, and this
 286 effect was evident in both directions (**Fig. 5B, C**). Of relevance, to validate that this impairment in
 287 communication specifically involves theta activity, we then ran the Granger analysis for all main
 288 EEG frequency domains (**Sup. Fig 1**). We observed that the flow of information between the
 289 tachogram and the EEG traces was affected only in the range of theta and unaltered in the other

290 windows. Thus, this data set suggests that the impairment of informational flow between heart
 291 and brain, caused by chronic and marked cardiac stress, can underlie the decrease of the theta
 292 rhythm at the central level.

293 3.4 TGAC8 mice display increased locomotor activity

294 Hippocampal theta activity is a crucial determinant of overall locomotor activity in species, such
 295 as mice²⁵. In particular, theta-1 (8-12 Hz) seems to be related to active movement and theta-2 (4-
 296 7 Hz) to alertness and immobility²⁶. Theta frequency is directly proportional to the animal velocity:
 297 slower oscillatory rhythms mean slower speed. Moreover, a regular theta rhythm also underpins
 298 a more stable and slower running speed during exploration²⁷. Thus, it is plausible that the decrease

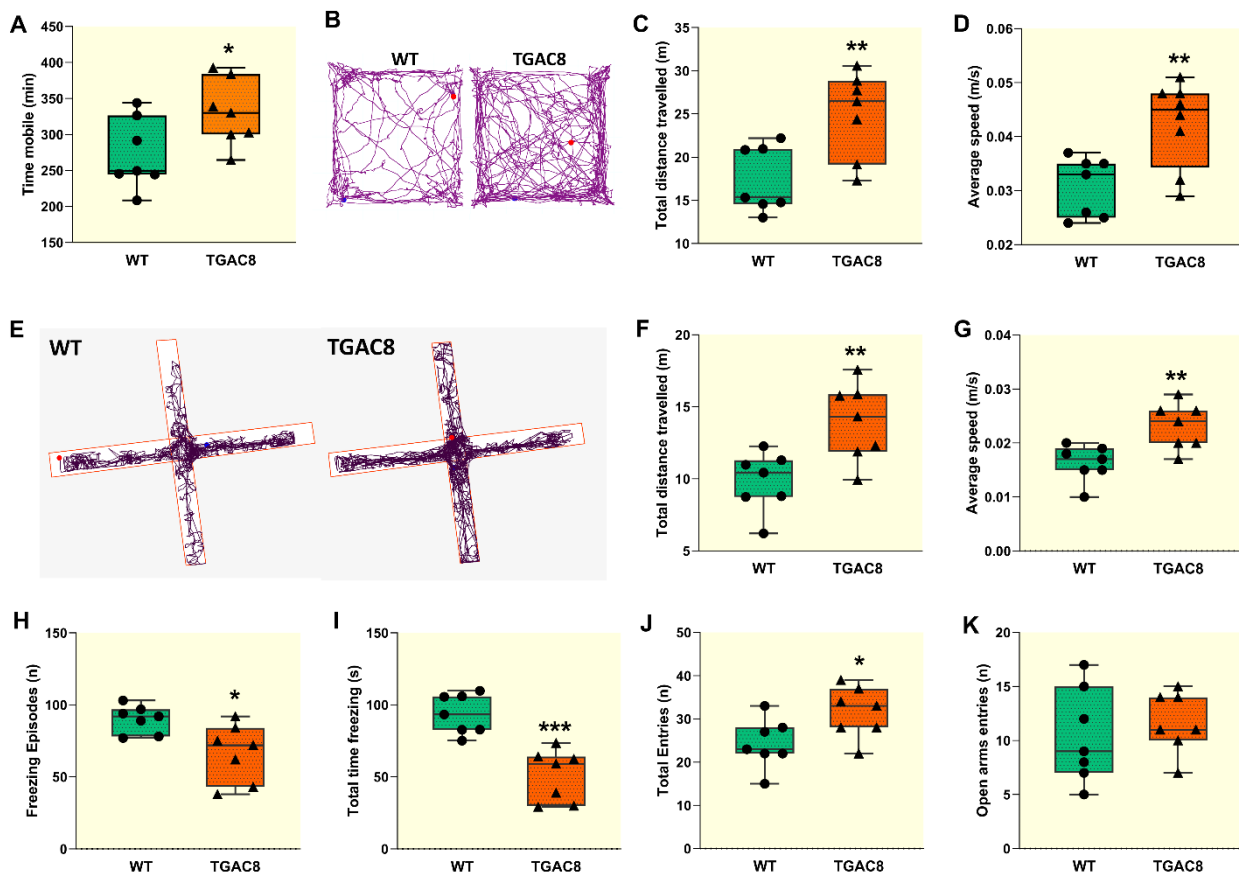


Figure 6 TGAC8 mice display a general increase in locomotor behavior. (A) Time mobile recorded trough actigraph; (B) Plot of the animals movements during OF test, WT vs TGAC8 mouse; (C) OF test, total distance travelled; (D) OF test, average speed; (E) Plot of the animals movements during EPM test, WT vs TGAC8 mouse; (F) EPM test, total distance travelled; (G) EPM test, average speed; (H) EPM test, freezing episodes; (I) EPM test, total time freezing; (J) EPM test, total entries in the arms of the labyrinth; (K) EPM test, number of entries in the open arms of the labyrinth. Results are shown as box and whiskers plot, N=7, unpaired t-test has been performed between WT and TGAC8 groups, * $p < 0.05$, ** $p < 0.01$, *** $p < 0.001$.

299 we observed in theta-2 activity in TGAC8s leads to changes in the behavioral phenotype of this
300 mouse. First, we assessed locomotor activity through a Holter actigraphy recording, open field,
301 and elevated plus maze test. We found a significant increase in all parameters linked to
302 locomotion in TGAC8 mice compared to age-matched littermates. For instance, compared to WT,
303 TGAC8 mice had heightened total time mobile in 24 hrs actigraphy (* $p < 0.05$, **Fig. 6A**). Consistent
304 with this finding, the open field (OF) test revealed that the transgenic mice traveled more and at

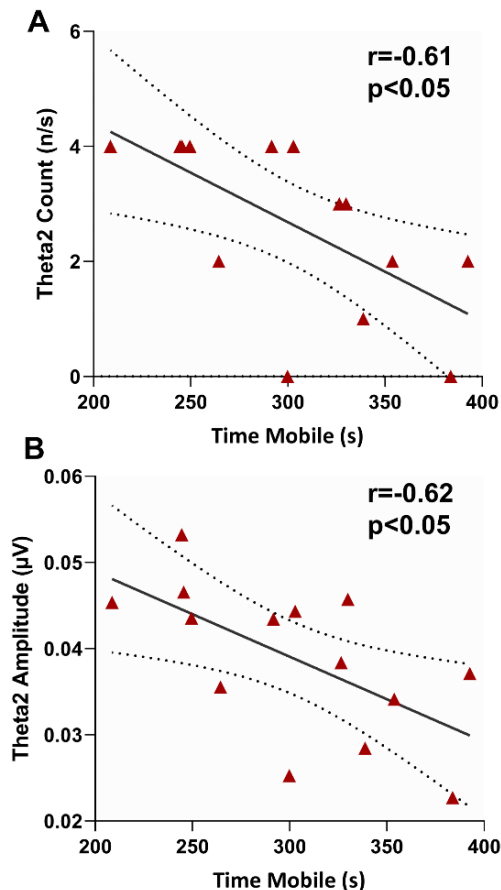


Figure 7 Time spent mobile correlates with theta-2 patterns. (A) Correlation between 24hrs time mobile and theta-2 waves count; (B) Correlation between 24hrs time mobile and theta-2 waves amplitude. Data are displayed in scatterplots; thick black lines represent the best linear fit through data; dotted lines represent two-tailed 95% confidence interval; text inset reports Pearson's Rho values and associated p-values.

a higher average speed than WT ones (+43% and +38%, respectively, $p < 0.01$) (**Fig. 6 C, D**). The elevated plus-maze (EPM) test also yielded consistent evidence, showing a significant difference in total distance traveled and average speed is present between TGAC8 and WT mice (** $p < 0.01$) (**Fig. 6F, G**). Of relevance, the transgenic strain also displayed a considerable decrease in episodes and time of freezing behavior (-25%, $p < 0.05$ and -45%, $p < 0.001$) (**Fig. 6H, I**). In keeping with the heightened locomotor activity, the total entries in the arms of the labyrinth were significantly increased in TGAC8, in the absence of changes in open arms entries (**Fig. 6J, K**). In aggregate, these findings indicate that under persistent chronotropic/inotropic stress and cardiac autonomic control escape, such as that occurring in TGAC8 mice, heightened locomotor activity occurs. To further validate this new notion, i.e., that in TGAC8 mice, locomotor behavior changes associate with theta-2 activity depletion, we correlated the time spent by the mice in mobile status with their theta

326 pattern. We observed that theta waves count was inversely proportional to the mobile time ($r = -$
327 0.61, $p < 0.05$) (**Fig. 7A**). We observed the same trend concerning theta amplitude, i.e., negative

328 correlation with time mobile ($r=-0.62$, $p<0.05$) (**Fig. 7B**). Hence, our data show that the decrease
 329 in theta-2 oscillatory rhythm is correlated to an overall increase in locomotor activity.

330 3.5 Cardiac AC8 overexpression does not affect anxiety, associative learning, and spatial 331 memory

332 Anxiety responses evoke irregular variations in the cardiac rhythm that can be perceived centrally
 333 as a state of danger^{28,29}. Conversely, here, we set out to determine whether in the context of
 334 chronically elevated heart-born sympathetic stress anxiety-like behavior is present in TGAC8. To

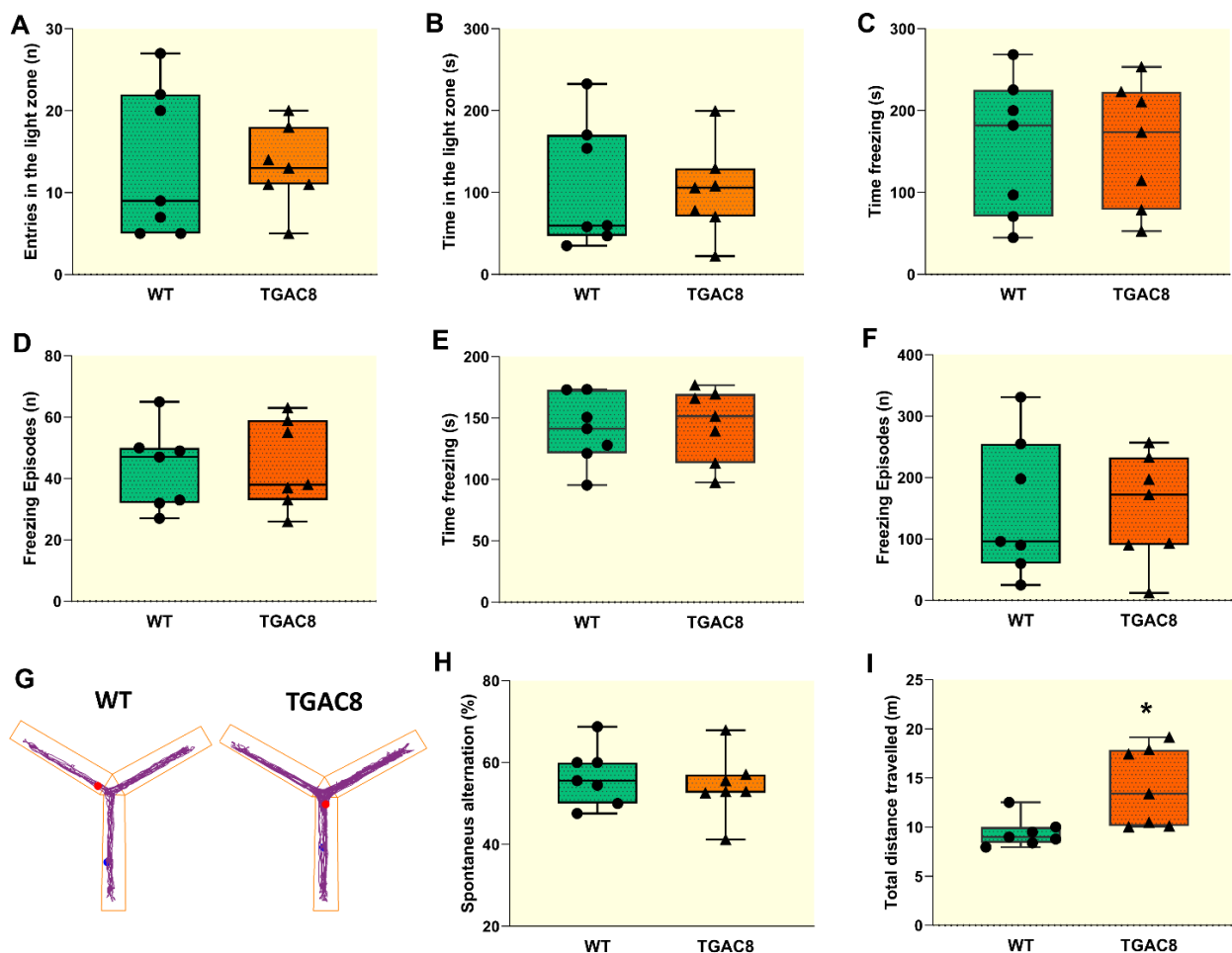


Figure 8. TGAC8 mice display a general increase in locomotor behavior not related to emotional or cognitive domains. (A) LDB test, number of entries in the light zone; (B) LDB test, time spent in the light zone; (C) Contextual FC test, time freezing; (D) Contextual FC, freezing episodes; (E) Cued FC, time freezing; (F) Cued FC, freezing episodes; (G) Plot of the animals movements during Y-maze test, WT vs TGAC8 mouse; (H) Y-maze test, percentage of spontaneous alternations; (I) Y-maze test, total distance travelled. Results are shown as box and whiskers plot, $N=7$, unpaired t-test has been performed between WT and TGAC8 groups, * $p<0.05$

335 sort this out, we first performed the EPM test that revealed no difference in entries in open arms
336 (**Fig. 6K**). This is a primary parameter that could be extrapolated from the EPM test to measure
337 fear of open spaces. However, the EPM test can be biased by possible changes in locomotor
338 activity. Hence, we next performed the light-dark Box test (LDB) to evaluate this possibility. Again,
339 no differences were evident between WT and TGAC8 mice when considering the two main
340 parameters of the trial, i.e., entries in the light zone and time in the light zone, thus confirming
341 lack of heightened anxiety-like behavior (**Fig. 8A, B**). Since TGAC8 mice displayed a marked
342 decrease in freezing behavior, we evaluated the reasons for such alteration, namely whether this
343 effect is dependent on abnormal locomotor activity or other behavioral domains. To answer this
344 question, we subjected mice to the fear conditioning test, in which the motor component is
345 minimal. Under these circumstances, there was no difference between the two groups (**Fig. 8 C-**
346 **F**). Finally, to exclude the possibility of enhancing locomotor activity in TGAC8 mice related to
347 perturbation of spatial memory and orientation in this mouse strain, we performed the Y-Maze
348 test that showed no differences in terms of spatial memory (**Fig. 8H**) but confirmed a substantial
349 increase in total distance traveled by the transgenic mice (**Fig. 8I**). Altogether, these data suggest
350 that the increase in locomotor activity in TGAC8 mice is not secondary to emotional or cognitive
351 abnormalities.

352 **Discussion**

353 Anxiety and mood disorders can affect the heart rhythm and its variability³⁰ chronically, and loss
354 of the top-down control of the heart rhythm is an emerging risk factor for adverse outcomes in
355 several forms of cardiovascular disease³¹. Less clear is whether and how altered heart rhythm,
356 contractility, and lack of autonomic control on cardiac function affects brain functioning/signaling
357 in a bottom-up modality. For the first time, our study shows that TGAC8 mice harboring persistent
358 cardiac-initiated (chronotropic/inotropic) stress display altered heart-brain communication as well
359 as EEG patterns modifications and behavioral changes, i.e., locomotor activity.

360 Beat-to-beat heart variability, determined by both intrinsic SAN pacemaker cell activity
361 and its autonomic modulation, is crucial for optimal heart function³². Indeed, loss of proper top-
362 down brain controls, taken as a whole, exerted on the cardiovascular system is implicated in CVD
363 progression. For instance, after myocardial infarction (MI), or other cardiac disorders, loss of HRV

364 denotes a lack of vagal control and represents a significant predictor of death in MI subjects³³.
365 Indeed, downsizing parasympathetic influence on heart function implies unremitting sympathetic
366 activation, eventually exacerbating myocardial dysfunction and remodeling^{34,35}. This autonomic
367 imbalance is also present in patients with severe neuropathies or transplanted heart⁶. It is also
368 worth noting that individuals with anxiety or depressive disorders display a reduction in HRV,
369 manifested as a lack of complexity on heart rhythm that is the signature of increased sympathetic
370 signaling, in this instance initiated in the brain, predisposing to a higher risk of cardiovascular
371 death³¹. Furthermore, after MI, patients become more prone to depression. In turn, this eventuality
372 further fuels post-MI mortality and chronic LV dysfunction in these subjects³⁶. Experimentally,
373 inducing depression via chronic mild stress³⁷ in rats heightens sympathetic activity and aggravates
374 LV remodeling after MI³⁸. In the same vein, in a murine model of arrhythmogenic cardiomyopathy,
375 anxiety induced by psychosocial stress increases mortality and remodeling³⁹.

376 The present study confirms that in TGAC8 mice, heart rate is increased, while LF and HF
377 power bands are reduced, according to reduced parasympathetic and sympathetic autonomic
378 controls acting on heart function¹⁰. What is more, the alpha coefficient from the DFA, a measure
379 of the RR time series autosimilarity, is significantly reduced in TGAC8 mice. Low alpha value is an
380 adverse prognostic index in patients with implantable cardioverter-defibrillators⁴⁰. This measure
381 is in line with the loss of complexity within the TGAC8 heart rhythm as highlighted with the
382 reduced multiscale entropy¹⁰, and it suggests accelerated cardiac aging or pathology⁴¹.

383 Brain-heart communication is bidirectional in nature^{42,43}. For this reason, we inquired
384 whether the marked cardiac-initiated heart rhythm abnormalities in TGAC8 are associated with
385 concurrent EEG changes in a bottom-up modality⁴. Here, we report that mice with persistently
386 elevated intrinsic heart rate associated with a markedly coherent rhythm, show altered EEG
387 patterns. In mammals, including humans, the theta oscillations are among the most solid and
388 regular rhythms in the brain⁴⁴. According to the dualistic theory, two pairs of theta rhythms can
389 be recognized in rodents, ranging from 4 to 12 Hz, theta 1 oscillations (in the 8-12 Hz band), and
390 theta 2 oscillations (in the 4-7 Hz band)^{26,45}. This distinction stems from the dependence on
391 cholinergic signaling and sensitivity to anesthetics, such as urethane. Theta-1 is atropine-resistant
392 and urethane-sensitive, whereas theta-2 is atropine-sensitive but urethane-resistant²⁶. Here, we

393 observed a marked reduction in the EEG power spectrum in the range of theta-2, associated with
394 a depletion of the wave's count and amplitude.

395 To further validate that the observed changes in EEG patterns derived from an alteration
396 in the signaling between the heart and the brain, we assessed the heart/brain bidirectional
397 communication using the Granger Causality approach. Past functional magnetic resonance
398 imaging studies have identified several structures, including the amygdala, hypothalamus, and the
399 areas belonging to the prefrontal cortex that causally interact with autonomic nervous system
400 outflow at rest^{46,47}. This study is critical because it highlights pivotal structures in the top-down
401 control of cardiac output; among these is the hippocampus, the main generator of the theta
402 activity we studied²⁶. However, the same study failed at identifying causal interactions in the
403 direction from heart to brain, probably due to the study limitation on the rest condition.
404 Notwithstanding, previous work on the heart-brain coupling evaluating the impact of different
405 levels of sedation on the heart-brain coupling indicated that activity in the thalamocortical circuits
406 appears to be influenced by variations in cardiac rhythm and that this influence increases with the
407 level of sedation. This finding is in line with evidence on the importance of visceral rhythms⁹,
408 including the cardiac one, in modulating brain activity during sleep⁴⁸. At variance, in this work, we
409 show for the first time that this coupling is bidirectionally effective also during active wakefulness
410 and that it tends to be less effective in the TGAC8 model in which the heart is genetically
411 uncoupled from the brain since birth.

412 To assess the physiological relevance of the altered heart-brain communication, we
413 evaluated possible behavioral adaptations in TGAC8s. In rodents, theta rhythms have been linked
414 to locomotor activity because it plays a pivotal role in controlling initiation of the movement⁴⁹ and
415 regulating locomotion speed^{50,27,51}. Bellesi and coworkers reported that reduced EEG theta power,
416 expressed in the frontal and parietal cortical areas of rats, increased their motor activity, especially
417 when EEG changes were more prominent⁵². Consistent with this view, theta-2 has been related to
418 a state of immobility and alertness, with a possible role in inhibiting voluntary movement.⁵³ On
419 this basis, we anticipated that locomotor behavior in TGAC8 could be affected by theta-2
420 reduction. Moreover, we speculate that the overall rise in locomotor activity is "functionally
421 justified" and congruent with the chronic peripheral physiological modification, such as the

422 increased heart rate. Indeed, the TGAC8 mouse heart experiences and must handle a status akin
423 to "perpetual exercise". At the same time, however, the brain needs to adapt its outflow, switching
424 the animal behavior from a state of rest to an active one, such as running, thus congruent with
425 the substantial increase of cardiac work experienced by TGAC8 mice. This phenomenon fits
426 perfectly with Damasio's theory of the somatic marker¹: the brain adapts and responds befittingly
427 to a stimulus detected in the periphery. Moreover, at least in our opinion, it is not surprising that
428 the behavioral phenotype observed in TGAC8 is characterized by an increase in locomotor activity
429 and not by a state of anxiety. Indeed, it is worth recalling that the cardiac chronotropic stress
430 experienced by the TGAC8 mice is regular and continuous, i.e., similar to a state of "perpetual
431 exercise". Conversely, the rhythm alterations that subtend anxiety typically come in sudden and
432 irregular bouts, often characterized by palpitations and arrhythmias^{54,55}. Actually, similar changes
433 in heart-brain communication occur in anticipation of exercise performance. Therefore, in this
434 instance, the brain signals to the heart to increase its beating rate prior to the actual start of the
435 physical effort⁵⁶. In the case of TGAC8 the situation is reverted and it is increased heart rate and
436 reduced HRV, born within the heart itself, that signal to the brain to start locomotor activity.

437 Persistent AC8 overexpression can be perceived as a limitation of the present study due
438 to the difficulty of pairing this genetic manipulation to specific clinical settings. However, such an
439 extreme mouse model served well to the purpose of disconnecting (at least partially) the heart
440 from the brain while subjecting the heart of the TGAC8s to perpetual intrinsic stress *in situ*. And
441 testing the latter's effects on central functions/behavioral patterns was precisely the primary goal
442 of the present research.

443 **Conclusions**

444 Our study shows that cardiac-born persistent sympathetic stress bidirectionally alters the
445 information flow between the heart and brain, indicating heart-initiated signaling to the brain,
446 which influences central physiological patterns associated with locomotion. These results provide
447 proof of concept that pathophysiology arising within the heart is penetrant enough to alter brain
448 functions, thus primary adaptive behavioral responses.

449

450 **Funding**

451 This research was supported in part by the Intramural research Program of the NIH, National
452 institute on Aging. This research was supported also by National Institutes of Health R01 (R01
453 HL136918).

454 **CRedit authorship contribution statement** **Jacopo Agrimi**: Conceptualization, Investigation,
455 Formal analysis, Writing – original draft; **Danilo Menicucci**: Formal analysis, Methodology, Writing
456 – original draft. **Marco Laurino**: Formal analysis, Methodology; **Chelsea D Mackey**: Investigation,
457 Formal analysis, Writing – review & editing; **Laila Hasnain**: Investigation; **Sneha Dodaballapur**:
458 Investigation; **Ross A McDevitt**: Investigation; **Donald B Hoover**: Investigation, Formal analysis,
459 Writing – review & editing; **Angelo Gemignani**: Conceptualization, Writing – original draft,
460 Supervision; **Nazareno Paolucci**: Conceptualization, Writing – original draft, Supervision; **Edward**
461 **G Lakatta**: Conceptualization, Writing – original draft, Supervision

462 **Declaration of competing interest**

463 The authors declare that they have no known competing financial interests or personal
464 relationships that could have appeared to influence the work reported in this paper.

465

466 **Bibliography**

467

- 468 (1) Bechara, A.; Damasio, H.; Damasio, A. R. Emotion, decision making and the orbitofrontal
469 cortex. *Cereb Cortex* **2000**, *10* (3), 295.
- 470 (2) Bechara, A.; Damasio, H.; Tranel, D.; Damasio, A. R. The Iowa Gambling Task and the
471 somatic marker hypothesis: some questions and answers. *Trends Cogn Sci* **2005**, *9* (4), 159.
- 472 (3) Armour, J. A. The little brain on the heart. *Cleve Clin J Med* **2007**, *74 Suppl 1*, S48.
- 473 (4) Buckley, U.; Shivkumar, K. Stress-induced cardiac arrhythmias: The heart-brain interaction.
474 *Trends Cardiovasc Med* **2016**, *26* (1), 78.
- 475 (5) Ardell, J. L.; Armour, J. A. Neurocardiology: Structure-Based Function. *Compr Physiol* **2016**,
476 *6* (4), 1635.
- 477 (6) Awad, M.; Czer, L. S.; Hou, M.; Golshani, S. S.; Goltche, M.; De Robertis, M.; Kittleson, M.;
478 Patel, J.; Azarbal, B.; Kransdorf, E. et al. Early Denervation and Later Reinnervation of the
479 Heart Following Cardiac Transplantation: A Review. *J Am Heart Assoc* **2016**, *5* (11).
- 480 (7) Grupper, A.; Gewirtz, H.; Kushwaha, S. Reinnervation post-heart transplantation. *Eur Heart*
481 *J* **2018**, *39* (20), 1799.

- 482 (8) Doering, L. V.; Chen, B.; Deng, M.; Mancini, D.; Kobashigawa, J.; Hickey, K. Perceived control
483 and health-related quality of life in heart transplant recipients. *Eur J Cardiovasc Nurs* **2018**,
484 *17* (6), 513.
- 485 (9) Azzalini, D.; Rebollo, I.; Tallon-Baudry, C. Visceral Signals Shape Brain Dynamics and
486 Cognition. *Trends Cogn Sci* **2019**, *23* (6), 488.
- 487 (10) Moen, J. M.; Matt, M. G.; Ramirez, C.; Tarasov, K. V.; Chakir, K.; Tarasova, Y. S.; Lukyanenko,
488 Y.; Tsutsui, K.; Monfredi, O.; Morrell, C. H. et al. Overexpression of a Neuronal Type Adenylyl
489 Cyclase (Type 8) in Sinoatrial Node Markedly Impacts Heart Rate and Rhythm. *Front*
490 *Neurosci* **2019**, *13*, 615.
- 491 (11) Lipskaia, L.; Defer, N.; Esposito, G.; Hajar, I.; Garel, M. C.; Rockman, H. A.; Hanoune, J.
492 Enhanced cardiac function in transgenic mice expressing a Ca(2+)-stimulated adenylyl
493 cyclase. *Circ Res* **2000**, *86* (7), 795.
- 494 (12) Hoover, D. B.; Ozment, T. R.; Wondergem, R.; Li, C.; Williams, D. L. Impaired heart rate
495 regulation and depression of cardiac chronotropic and dromotropic function in
496 polymicrobial sepsis. *Shock* **2015**, *43* (2), 185.
- 497 (13) Wan, R.; Camandola, S.; Mattson, M. P. Intermittent food deprivation improves
498 cardiovascular and neuroendocrine responses to stress in rats. *J Nutr* **2003**, *133* (6), 1921.
- 499 (14) Kantz, H., and Schreiber, T *Nonlinear Time Series Analysis*; (Cambridge UK: Cambridge
500 University Press). 2004.
- 501 (15) Ferrarelli, F.; Huber, R.; Peterson, M. J.; Massimini, M.; Murphy, M.; Riedner, B. A.; Watson,
502 A.; Bria, P.; Tononi, G. Reduced sleep spindle activity in schizophrenia patients. *Am J*
503 *Psychiatry* **2007**, *164* (3), 483.
- 504 (16) Seth, A. K. A MATLAB toolbox for Granger causal connectivity analysis. *J Neurosci Methods*
505 **2010**, *186* (2), 262.
- 506 (17) T., K. D. P. P. S. P. S. Y. Testing the null hypothesis of stationarity against the alternative of
507 a unit root: How sure are we that economic time series have a unit root? *J. Econometrics*
508 **1992**, *54*, 159.
- 509 (18) Barrett, A. B.; Murphy, M.; Bruno, M. A.; Noirhomme, Q.; Boly, M.; Laureys, S.; Seth, A. K.
510 Granger causality analysis of steady-state electroencephalographic signals during
511 propofol-induced anaesthesia. *PLoS One* **2012**, *7* (1), e29072.
- 512 (19) Ding, M.; Bressler, S. L.; Yang, W.; Liang, H. Short-window spectral analysis of cortical event-
513 related potentials by adaptive multivariate autoregressive modeling: data preprocessing,
514 model validation, and variability assessment. *Biol Cybern* **2000**, *83* (1), 35.
- 515 (20) Sestakova, N.; Puzserova, A.; Kluknavsky, M.; Bernatova, I. Determination of motor activity
516 and anxiety-related behaviour in rodents: methodological aspects and role of nitric oxide.
517 *Interdiscip Toxicol* **2013**, *6* (3), 126.
- 518 (21) Bourin, M.; Hascoet, M. The mouse light/dark box test. *Eur J Pharmacol* **2003**, *463* (1-3),
519 55.
- 520 (22) Shoji, H.; Takao, K.; Hattori, S.; Miyakawa, T. Contextual and cued fear conditioning test
521 using a video analyzing system in mice. *J Vis Exp* **2014**, DOI:10.3791/50871
522 10.3791/50871(85).
- 523 (23) Kraeuter, A. K.; Guest, P. C.; Sarnyai, Z. The Y-Maze for Assessment of Spatial Working and
524 Reference Memory in Mice. *Methods Mol Biol* **2019**, *1916*, 105.

- 525 (24) Muller, A.; Kraemer, J. F.; Penzel, T.; Bonnemeier, H.; Kurths, J.; Wessel, N. Causality in
526 physiological signals. *Physiol Meas* **2016**, *37* (5), R46.
- 527 (25) Slawinska, U.; Kasicki, S. The frequency of rat's hippocampal theta rhythm is related to the
528 speed of locomotion. *Brain Res* **1998**, *796* (1-2), 327.
- 529 (26) Mikulovic, S.; Restrepo, C. E.; Siwani, S.; Bauer, P.; Pupe, S.; Tort, A. B. L.; Kullander, K.; Leao,
530 R. N. Ventral hippocampal OLM cells control type 2 theta oscillations and response to
531 predator odor. *Nat Commun* **2018**, *9* (1), 3638.
- 532 (27) Bender, F.; Gorbati, M.; Cadavieco, M. C.; Denisova, N.; Gao, X.; Holman, C.; Korotkova, T.;
533 Ponomarenko, A. Theta oscillations regulate the speed of locomotion via a hippocampus
534 to lateral septum pathway. *Nat Commun* **2015**, *6*, 8521.
- 535 (28) Schandry, R. Heart beat perception and emotional experience. *Psychophysiology* **1981**, *18*
536 (4), 483.
- 537 (29) Trotman, G. P.; Veldhuijzen van Zanten, J.; Davies, J.; Moller, C.; Ginty, A. T.; Williams, S. E.
538 Associations between heart rate, perceived heart rate, and anxiety during acute
539 psychological stress. *Anxiety Stress Coping* **2019**, *32* (6), 711.
- 540 (30) Hartmann, R.; Schmidt, F. M.; Sander, C.; Hegerl, U. Heart Rate Variability as Indicator of
541 Clinical State in Depression. *Front Psychiatry* **2018**, *9*, 735.
- 542 (31) Gorman, J. M.; Sloan, R. P. Heart rate variability in depressive and anxiety disorders. *Am*
543 *Heart J* **2000**, *140* (4 Suppl), 77.
- 544 (32) Singh, N.; Moneghetti, K. J.; Christle, J. W.; Hadley, D.; Plews, D.; Froelicher, V. Heart Rate
545 Variability: An Old Metric with New Meaning in the Era of using mHealth Technologies for
546 Health and Exercise Training Guidance. Part One: Physiology and Methods. *Arrhythm*
547 *Electrophysiol Rev* **2018**, *7* (3), 193.
- 548 (33) Buccelletti, E.; Gilardi, E.; Scaini, E.; Galiuto, L.; Persiani, R.; Biondi, A.; Basile, F.; Silveri, N. G.
549 Heart rate variability and myocardial infarction: systematic literature review and
550 metanalysis. *Eur Rev Med Pharmacol Sci* **2009**, *13* (4), 299.
- 551 (34) Hanna, P.; Shivkumar, K.; Ardell, J. L. Calming the Nervous Heart: Autonomic Therapies in
552 Heart Failure. *Card Fail Rev* **2018**, *4* (2), 92.
- 553 (35) Barboza, C. A.; Fukushima, A. R.; Carrozzi, N.; Machi, J. F.; Dourado, P. M. M.; Mostarda, C.
554 T.; Irigoyen, M. C.; Nathanson, L.; Morris, M.; Caperuto, E. C. et al. Cholinergic Stimulation
555 by Pyridostigmine Bromide Before Myocardial Infarction Prevent Cardiac and Autonomic
556 Dysfunction. *Sci Rep* **2019**, *9* (1), 2481.
- 557 (36) Ziegelstein, R. C. Depression after myocardial infarction. *Cardiol Rev* **2001**, *9* (1), 45.
- 558 (37) Gronli, J.; Murison, R.; Fiske, E.; Bjorvatn, B.; Sorensen, E.; Portas, C. M.; Ursin, R. Effects of
559 chronic mild stress on sexual behavior, locomotor activity and consumption of sucrose and
560 saccharine solutions. *Physiol Behav* **2005**, *84* (4), 571.
- 561 (38) Shi, S.; Liang, J.; Liu, T.; Yuan, X.; Ruan, B.; Sun, L.; Tang, Y.; Yang, B.; Hu, D.; Huang, C.
562 Depression increases sympathetic activity and exacerbates myocardial remodeling after
563 myocardial infarction: evidence from an animal experiment. *PLoS One* **2014**, *9* (7), e101734.
- 564 (39) Agrimi, J.; Scalco, A.; Agafonova, J.; Williams Iii, L.; Pansari, N.; Keceli, G.; Jun, S.; Wang, N.;
565 Mastorci, F.; Tichnell, C. et al. Psychosocial Stress Hastens Disease Progression and Sudden
566 Death in Mice with Arrhythmogenic Cardiomyopathy. *J Clin Med* **2020**, *9* (12).

- 567 (40) Perkiomaki, J. S.; Zareba, W.; Daubert, J. P.; Couderc, J. P.; Corsello, A.; Kremer, K. Fractal
568 correlation properties of heart rate dynamics and adverse events in patients with
569 implantable cardioverter-defibrillators. *Am J Cardiol* **2001**, *88* (1), 17.
- 570 (41) Yaniv, Y.; Ahmet, I.; Tsutsui, K.; Behar, J.; Moen, J. M.; Okamoto, Y.; Guiriba, T. R.; Liu, J.;
571 Bychkov, R.; Lakatta, E. G. Deterioration of autonomic neuronal receptor signaling and
572 mechanisms intrinsic to heart pacemaker cells contribute to age-associated alterations in
573 heart rate variability in vivo. *Aging Cell* **2016**, *15* (4), 716.
- 574 (42) Habecker, B. A.; Anderson, M. E.; Birren, S. J.; Fukuda, K.; Herring, N.; Hoover, D. B.;
575 Kanazawa, H.; Paterson, D. J.; Ripplinger, C. M. Molecular and cellular neurocardiology:
576 development, and cellular and molecular adaptations to heart disease. *J Physiol* **2016**, *594*
577 (14), 3853.
- 578 (43) Agrimi, J.; Spalletti, C.; Baroni, C.; Keceli, G.; Zhu, G.; Caragnano, A.; Matteucci, M.; Chelko,
579 S.; Ramirez-Correa, G. A.; Bedja, D. et al. Obese mice exposed to psychosocial stress display
580 cardiac and hippocampal dysfunction associated with local brain-derived neurotrophic
581 factor depletion. *EBioMedicine* **2019**, *47*, 384.
- 582 (44) O'Keefe, J. Hippocampus, theta, and spatial memory. *Curr Opin Neurobiol* **1993**, *3* (6), 917.
- 583 (45) Muller, R.; Struck, H.; Ho, M. S.; Brockhaus-Dumke, A.; Klosterkötter, J.; Broich, K.; Hescheler,
584 J.; Schneider, T.; Weiergraber, M. Atropine-sensitive hippocampal theta oscillations are
585 mediated by Cav2.3 R-type Ca(2)(+) channels. *Neuroscience* **2012**, *205*, 125.
- 586 (46) Duggento, A.; Bianciardi, M.; Passamonti, L.; Wald, L. L.; Guerrisi, M.; Barbieri, R.; Toschi, N.
587 Globally conditioned Granger causality in brain-brain and brain-heart interactions: a
588 combined heart rate variability/ultra-high-field (7 T) functional magnetic resonance
589 imaging study. *Philos Trans A Math Phys Eng Sci* **2016**, *374* (2067).
- 590 (47) Valenza, G.; Sclocco, R.; Duggento, A.; Passamonti, L.; Napadow, V.; Barbieri, R.; Toschi, N.
591 The central autonomic network at rest: Uncovering functional MRI correlates of time-
592 varying autonomic outflow. *Neuroimage* **2019**, *197*, 383.
- 593 (48) Pigarev, I. N.; Pigareva, M. L. The state of sleep and the current brain paradigm. *Front Syst*
594 *Neurosci* **2015**, *9*, 139.
- 595 (49) Nunez, A.; Buno, W. The Theta Rhythm of the Hippocampus: From Neuronal and Circuit
596 Mechanisms to Behavior. *Front Cell Neurosci* **2021**, *15*, 649262.
- 597 (50) Bland, B. H.; Oddie, S. D. Theta band oscillation and synchrony in the hippocampal
598 formation and associated structures: the case for its role in sensorimotor integration.
599 *Behav Brain Res* **2001**, *127* (1-2), 119.
- 600 (51) Long, L. L.; Hinman, J. R.; Chen, C. M.; Escabi, M. A.; Chrobak, J. J. Theta dynamics in rat:
601 speed and acceleration across the Septotemporal axis. *PLoS One* **2014**, *9* (5), e97987.
- 602 (52) Bellesi, M.; Vyazovskiy, V. V.; Tononi, G.; Cirelli, C.; Conti, F. Reduction of EEG theta power
603 and changes in motor activity in rats treated with ceftriaxone. *PLoS One* **2012**, *7* (3),
604 e34139.
- 605 (53) Pscherer, C.; Muckschel, M.; Summerer, L.; Bluschke, A.; Beste, C. On the relevance of EEG
606 resting theta activity for the neurophysiological dynamics underlying motor inhibitory
607 control. *Hum Brain Mapp* **2019**, *40* (14), 4253.
- 608 (54) Abbott, A. V. Diagnostic approach to palpitations. *Am Fam Physician* **2005**, *71* (4), 743.
- 609 (55) Carnevali, L.; Trombini, M.; Graiani, G.; Madeddu, D.; Quaini, F.; Landgraf, R.; Neumann, I.
610 D.; Nalivaiko, E.; Sgoifo, A. Low vagally-mediated heart rate variability and increased

611 susceptibility to ventricular arrhythmias in rats bred for high anxiety. *Physiol Behav* **2014**,
612 128, 16.
613 (56) Brown, R.; Kemp, U.; Macefield, V. Increases in muscle sympathetic nerve activity, heart
614 rate, respiration, and skin blood flow during passive viewing of exercise. *Front Neurosci*
615 **2013**, 7, 102.
616